Hard Diffraction at the TEVATRON

Kristal Mauritz[1] for the DØ and CDF Collaborations

Iowa State University, Ames IA 50011, USA

Abstract. Experimental results on hard diffraction with the CDF and DØ detectors at the Fermilab TEVATRON are reviewed and compared with theoretical expectations.

1 Introduction

Diffractive and elastic events have been studied for over 30 years and are responsible for about 40% of the $p\overline{p}$ cross-section, but still much is unknown about the nature of the process. In addition to the diffractively scattered proton or antiproton, they are characterized by the complete, or nearly complete, absence of hadronic particle activity over a large rapidity or pseudorapidity region [1,2]. This region is called a 'rapidity gap' and in elastic $p\overline{p}$ scattering, the 'rapidity gap' is complete and extends over the whole kinematically allowed rapidity range. Single diffraction is the break-up of the p or $\overline{p}$ into a typically low-mass 'diffractive system' at low momentum transfer generally assumed to be a spin-1/2 nucleon resonance with the quantum numbers of the proton. The concept of a "Pomeron" was invented by Pomeranchuk to explain this diffractive process in the context of Regge theory [3]. The pomeron, which is a color-singlet with quantum numbers of the vacuum, is the exchanged object presumed to produce a diffractive event.

Hard single diffraction (HSD) was introduced by Ingelman and Schlein[4] in 1985 as a model to probe the pomeron. The event is treated in a factorizable way, i.e. the pomeron is "emitted" by the anti-proton (or proton) with a certain probability or flux and then struck by the other proton (or antiproton) with a high p_T. 'Hard' diffraction constitutes a larger tranverse momentum process in addition to the diffractive scattering. The events studied here have a hard scattered system of at least two jets with an $E_T \geq 7\,\mathrm{GeV}$ (usually higher) as well as a rapidity gap. The first experimental results on the subject were published by the UA8 Collaboration, which showed the existence of jets in single diffractive events and that these jets had rapidity and longitudinal momentum distributions consistent with a hard pomeron structure [5]. The field of study has expanded dramatically since then. Recent results from HERA and the TEVATRON include studies of deep inelastic scattering in large rapidity gap events [6], diffractive jet production [7–10] and diffractive W-boson production [11]. Measurements at both HERA and the TEVATRON are consistent with a predominantly gluonic pomeron, but measured rates at the TEVATRON are several times lower than

predictions based on HERA data[12]. The combination of these results gives new insight into the exchanged object.

This paper will provide an introduction and brief review on the recent results at the TEVATRON of hard single diffraction and hard double pomeron exchange. Studies of hard diffraction can be used to increase our knowledge of the structure of the pomeron, especially when combined with complementary hard diffractive measurements at HERA. They can also test such basic assumptions as to the very nature of the pomeron as a particle-like object.

1.1 Hard Diffraction at the TEVATRON

At the TEVATRON, there are three types of hard diffractive processes accessible to experimentation: hard single diffraction, double diffraction or hard color singlet exchange (HCS), and hard double pomeron exchange (DPE). Hard single diffractive jet production is a subset of single diffraction with a hard scatter in the final state. Figure 1(a) shows a two-jets final state in the process $p + \overline{p} \rightarrow j + j + X$. Because the pomeron is a color-singlet, particle production is typically suppressed between the outgoing hadron and the jets and a forward rapidity gap results in these events. Hard color singlet exchange (Fig. 1b) is a double diffractive process, but at large t, which produces a final state of a rapidity gap between jets. To produce a rapidity gap, the exchanged particle must again be a color-singlet, but the event rates are too large to be explained by electroweak boson exchange and indicate a strong interaction process [13].

Another type of diffractive event is double pomeron exchange (DPE), characterized by particle production only in the central rapidity region (Fig. 1c). Each incoming hadron 'emits' a (or interacts via an internal) pomeron (state) leading to large forward and backward rapidity gaps, and the interaction of the two pomerons results in central particle production. This class of events was first observed at the ISR in

$$\mathrm{pp} \rightarrow \mathrm{pp}\pi^+\pi^- \tag{1}$$

interactions [14]. At the ISR there was insufficient energy to produce hard scattering in DPE events. UA1 previously has made attempts to find "hard double pomeron exchange" using central particle production and forward rapidity

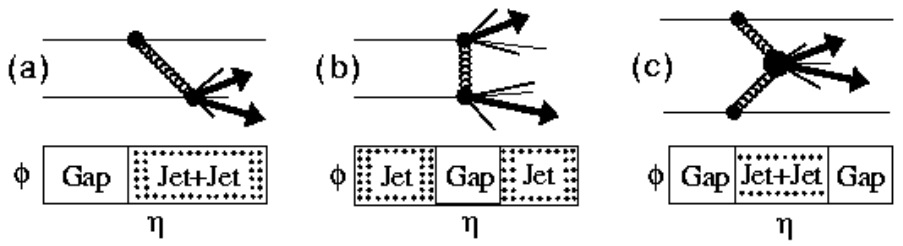

Fig. 1. Event topology of dijet production in (a) single diffraction, (b) hard color singlet, and (c) hard double pomeron exchange.

gaps [15]. Although they did find a class of events consistent with double pomeron exchange, they were unable to show that these events did not arise from multiplicity fluctuations in color exchange jet events.

All three classes of events can be tagged by the rapidity gap signature. HSD and DPE can also be tagged by detecting the leading particle(s) on the gap side. Using rapidity gap tagging, the CDF and DØ collaborations have studied dijet production (two or more jets) in all three processes at $\sqrt{s} = 1800\,\mathrm{GeV}$. In addition, CDF has studied (single) diffractive W-boson, b-quark, and J/ψ production using rapidity gaps, and dijet production in HSD and DPE using a "roman pot" magnetic spectrometer to detect leading antiprotons [16]. DØ has also studied all three processes at $\sqrt{s} = 630\,\mathrm{GeV}$ and made measurements of HSD with different jet locations [17].

2 Hard Single Diffraction

CDF [18] and DØ [19] measure the rate of single diffraction in different processes as the fraction of events with forward rapidity gaps, called the gap fraction. The rapidity gaps are identified by measuring the multiplicity in the forward detectors: the calorimeter and the forward scintillator arrays. Both experiments tag rapidity gaps using the forward calorimeters ($2.4 < |\eta| < 4.2$ at CDF and $3.0 < |\eta| < 5.2$ at DØ) and the forward scintillator arrays, called the beam-beam counter (BBC) at CDF ($3.2 < |\eta| < 5.9$) and the LevelØ (LØ) detector at DØ ($2.3 < |\eta| < 4.3$). A particle is tagged by a hit in the scintillation counters or by the deposition of energy in a calorimeter tower greater than a certain threshold energy, set to just above the noise to maximize the sensitivity to particles. At CDF, this threshold is 1500 MeV per calorimeter tower, and at DØ it is 150 MeV in an electromagnetic calorimeter tower or 500 MeV in a hadronic calorimeter tower.

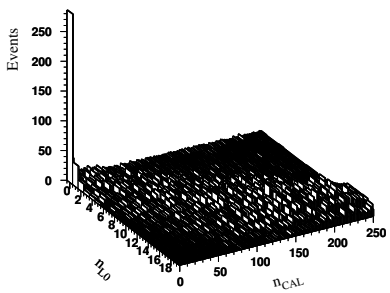

Fig. 2. DØ multiplicity distribution for 1800 GeV forward jet events.

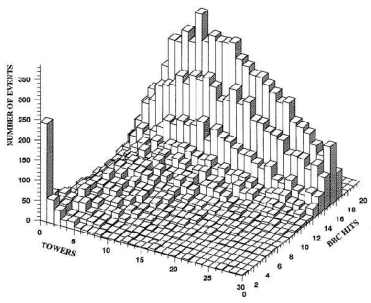

Fig. 3. CDF multiplicity distribution for 1800 GeV forward jet events.

Figures 2 and 3, respectively, show sample multiplicity distributions at DØ and CDF. The number of calorimeter towers (n_{CAL} or towers) above the energy

threshold and the number of scintillator hits (n_{L0} or BBC) are measured opposite the leading two jets for the forward jet trigger (at least two jets with $E_T > 12\,\mathrm{GeV}$ and $|\eta| > 1.6$ for DØ or $E_T > 20\,\mathrm{GeV}$ and $1.8 < |\eta| < 3.5$ for CDF). The distributions show the characteristic peak at zero multiplicity in qualitative agreement with expectations for a diffractive signal component and a higher multiplicity distribution associated with non-diffractive, background events. The diffractive and non-diffractive peaks at DØ are more separated because of the lower threshold and finer calorimeter segmentation. Both experiments fit the distributions to extract the gap fraction, the number of diffractive events divided by the total number of events in the sample. CDF fits the two-dimensional multiplicity distribution to a line along the diagonal and DØ simultaneously fits the diffractive signal to a falling exponential and the background to a four-parameter fit.

Table 1. Diffractive to total production ratios at the TEVATRON

SD hard process	$\sqrt{s}$ (GeV)	$R = \frac{\mathrm{DIFF}}{\mathrm{TOTAL}}$ (%)	Comments	Exp't
$W(\to e\nu)$	1800	$(1.15 \pm 0.55)^* \mathcal{A}^\dagger$	$E_T^e, \not\!\!E_T > 20$ GeV	CDF [11]
Forward Jets	1800	$(0.75 \pm 0.10)^* \mathcal{A}^\dagger$	$E_T^{jet} > 20$ GeV, $\eta^{jet} > 1.8$	CDF [8]
Forward Jets	1800	0.65 ± 0.04	$E_T^{jet} > 12$ GeV, $\eta^{jet} > 1.6$	DØ*
Forward Jets	630	1.19 ± 0.08	$E_T^{jet} > 12$ GeV, $\eta^{jet} > 1.6$	DØ*
Central Jets	1800	0.22 ± 0.05	$E_T^{jet} > 15$ GeV, $\eta^{jet} < 1.0$	DØ*
Central Jets	630	0.90 ± 0.06	$E_T^{jet} > 12$ GeV, $\eta^{jet} < 1.0$	DØ*
$b(\to e + X)$	1800	$(0.62 \pm 0.25)^* \mathcal{A}^\dagger$	$\mid \eta^e \mid < 1.1$, $9.5 < p_T^e < 20$ GeV	CDF [20]
$J/\psi(\to \mu\mu)$	1800	0.64 ± 0.12	$\mid \eta^\mu \mid < 0.6$, $p_T^\mu > 2$ GeV	CDF*

* Preliminary
$\mathcal{A}^\dagger$ Includes rapidity gap acceptance based on a hard gluon structure function

Table 1 shows the measured gap fractions at both experiments for final state forward jet, central jet, W-boson, J/ψ, and b-quark production. There are several notable observations:

- All gap fractions for hard single diffraction are $\sim O(1\%)$.
- Forward jet gap fractions > central jet gap fractions.
- Gap fractions at $\sqrt{s} = 630\,\mathrm{GeV}$ are at least twice as large as the gap fractions at $\sqrt{s} = 1800\,\mathrm{GeV}$.

As can be seen by the $\mathcal{A}^\dagger$ in the gap fraction measurements in Table 1, the two experiments treat the measurement of the rate for hard diffraction slightly differently. To understand this, it is important to look at the phenomenology.

2.1 Phenomenology

The theory of diffraction relies on phenomenological models. The Ingelman-Schlein model supposed that the pomeron is a composite pseudoparticle, composed of quarks and gluons. They proposed several simple structure functions and calculated the cross-section for hard diffraction as the probability of a pomeron being 'emitted' (called the flux factor) with the QCD hard matrix element. The diffractive Monte Carlo POMPYT 2.6 [21] is based on the IS model and assumes a pomeron is emitted from the proton. The standard Donnachie-Landshoff flux factor is used at both experiments, and the results can be easily rescaled for different flux factors. It allows for several possible choices of a presumed pomeron structure function, $s(x)$. The four main structure choices are a: (i) 'hard gluon', a pomeron consisting of two gluon exchange, $s(x) \propto x(1-x)$; (ii) 'flat gluon', $s(x) \propto$ constant; (iii) 'quark', a pomeron consisting of two light quarks, $s(x) \propto x(1-x)$; and (iv) 'soft gluon', with a gluon distribution similar to that in the proton, $s(x) \propto (1-x)^5$. The pomeron takes a small fraction of the proton's momentum called ξ, and a parton in the pomeron with a momentum fraction β to interact in the hard scattering.

The corresponding diffractive Monte Carlo multiplicity distributions with POMPYT show the same characteristic peak at low multiplicities as observed in the diffractive data with a tail extending to larger multiplicities that is dependent on the structure function choice. The expected fraction of diffractive events that are produced with a rapidity gap, called the rapidity gap acceptance, can be calculated for each structure function. The rapidity gap acceptance is treated differently between the two experiments. CDF assumes a hard gluon structure function (which has its basis in HERA data) and folds the acceptance into the data gap fraction to provide a "true" diffractive rate. DØ chooses to measure the rapidity gap fraction with no model dependence and folds the gap acceptance into the Monte Carlo predictions. For comparison, the DØ 1800 GeV forward jets gap fraction with a hard gluon gap efficiency increases the preliminary "measured" gap fraction to $(0.88 \pm 0.05)\%$.

2.2 DØ Analysis

The gap fraction can be calculated from Monte Carlo as the ratio of the number of rapidity gap events using POMPYT to the number of non-diffractive events with PYTHIA 5.7 [22] divided by the gap acceptance. The Monte Carlo gap fractions are shown in Table 2, and the trend is for the harder gluon rates to be much higher than the data, although the different data sets do not favor a particular $\sqrt{s}$-dependent scale factor as suggested by Ref. [23].

In the gap fraction ratios also shown in Table 2, the flux factor cancels for the same $\sqrt{s}$, while for different $\sqrt{s}$, any dependence on the flux factor is reduced. The Monte Carlo 630/1800 ratios are in much better agreement with the data than the numerator and denominator separately. However, the hard and flat gluon structures, which have been favored by previous measurements, are inconsistent with the forward/central jet ratio, despite the full cancellation of the flux factor.

For a gluon dominated pomeron to describe the data, the addition of a significant soft gluon component, which rarely produces central jet events with rapidity gaps, would be required.

Table 2. The DØ preliminary measured and predicted gap fractions and ratios.

	Gap Fraction				
Sample	Data	Hard Gluon	Flat Gluon	Soft Gluon	Quark
1800 GeV $\|\eta\| > 1.6$	$0.65\% + 0.04\% - 0.04\%$	$2.2\% \pm 0.3\%$	$2.2\% \pm 0.3\%$	$1.4\% \pm 0.2\%$	$0.79\% \pm 0.12\%$
1800 GeV $\|\eta\| < 1.0$	$0.22\% + 0.05\% - 0.04\%$	$2.5\% \pm 0.4\%$	$3.5\% \pm 0.5\%$	$0.05\% \pm 0.02\%$	$0.49\% \pm 0.06\%$
630 GeV $\|\eta\| > 1.6$	$1.19\% + 0.08\% - 0.08\%$	$3.9\% \pm 0.9\%$	$3.1\% \pm 0.8\%$	$1.9\% \pm 0.4\%$	$2.2\% \pm 0.5\%$
630 GeV $\|\eta\| < 1.0$	$0.90\% + 0.06\% - 0.06\%$	$5.2\% \pm 0.7\%$	$6.3\% \pm 0.9\%$	$0.13\% \pm 0.11\%$	$1.6\% \pm 0.2\%$
	Gap Fraction Ratio				
630/1800 FWD JET	$1.8 + 0.2 - 0.2$	1.7 ± 0.4	1.4 ± 0.3	1.4 ± 0.3	2.7 ± 0.6
630/1800 CEN JET	$4.1 + 0.8 - 1.0$	2.1 ± 0.4	1.8 ± 0.3	2.7 ± 2.4	3.2 ± 0.5
1800 FWD/CEN JET	$3.0 + 0.7 - 0.7$	0.88 ± 0.18	0.64 ± 0.12	$29. \pm 11.$	1.6 ± 0.3
630 FWD/CEN JET	$1.3 + 0.1 - 0.1$	0.75 ± 0.16	0.48 ± 0.12	$15. \pm 12.$	1.4 ± 0.3

DØ also uses an inclusive jet trigger in coincidence with a rapidity gap in the LØ detector to obtain a large number of low background single diffractive candidate events with which to study the event characteristics. After reinforcing the rapidity gap in the calorimeter, the number of jets, jet width, $\delta\phi$, and E_T of the leading two jets are shown in figure 4 for 1800 GeV diffractive (solid) and non-diffractive (dashed) central jet events. The diffractive events are consistent with less overall radiation than the non-diffractive events, and the E_T distributions are similar.

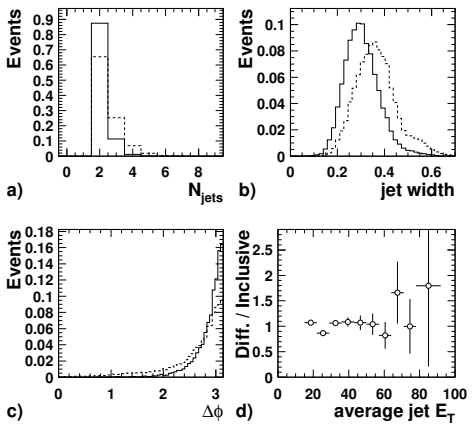

Fig. 4. The number of jets, jet width, $\delta\phi$ between jets, and the E_T distribution for the two central leading jets at 1800 GeV for the diffractive (*solid line*) and non-diffractive (*dashed line*) events (DØ preliminary)

The ξ distribution, or the momentum loss of the diffracted proton, can also be calculated using [24]

$$\xi \approx \Sigma \frac{E_{T_i} e^{\eta_i}}{\sqrt{s}}, \tag{2}$$

summing over the particles with the highest η and largest E_T. The outgoing diffracted proton (or the rapidity gap) is defined to be at positive η. This formula measures ξ using only the calorimeter, emphasizing the well-measured central region close the gap. It contains no model-dependence, and it can be defined even for non-diffractive events. After correcting for energy scale differences between Monte Carlo and data, the ξ distribution (solid) for 1800 GeV and 630 GeV forward and central jets are shown in Figure 5. The dotted and dashed curves reflect the high and low error.

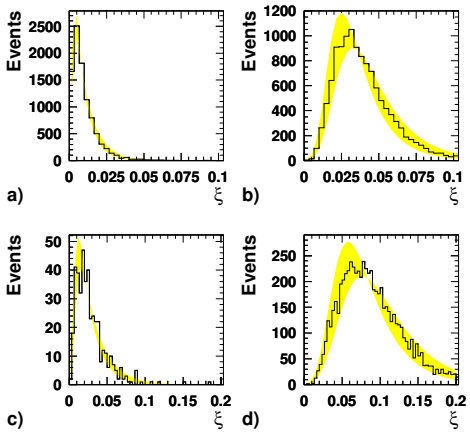

Fig. 5. The ξ distribution (*solid line*) and one sigma uncertainty for a)-b) $\sqrt{s}$ = 1800 GeV and c)-d) $\sqrt{s}$ = 630 GeV forward and central jets (DØ preliminary)

The forward jet ξ distribution at both 1800 and 630 GeV is peaked toward lower values of ξ although separated from zero because the pomeron requires a certain amount of momentum to create two 12 GeV jets. The central jet ξ distribution is spread over higher values, consistent with the pomeron requiring more momentum to balance the parton in the non-diffracted (anti)proton. The ξ distribution at 630 GeV is higher overall than at 1800 GeV, as expected because more momentum is needed from the pomeron at lower $\sqrt{s}$ with the same jet requirements. Although the trends of the ξ distribution are consistent with expectations, pomeron exchange is typically thought to dominate for very low values of $\xi < 0.05$. The large values of ξ observed, however, can be reproduced well with Monte Carlo.

2.3 CDF Analysis

The gluon content of the diffractive structure function is measured at CDF by comparing the hard single diffractive rates for final states with different sensitivity to quarks and gluons. This is similar to what is done by ZEUS, whith compares the diffractive deep inelastic scattering (D-DIS) to dijet photoproduction rates, and by H1, through a QCD analysis of the Q^2 evolution of the diffractive structure function measured in D-DIS. Both experiments measure a high gluon content. CDF measured, with the W and dijet production rates, a gluon fraction of $f_g = 0.7 \pm 0.2$ [11], and has a new measurement including the b-quark production rate of $f_g = 0.54^{+0.16}_{-0.14}$ [20] (see Fig 6).

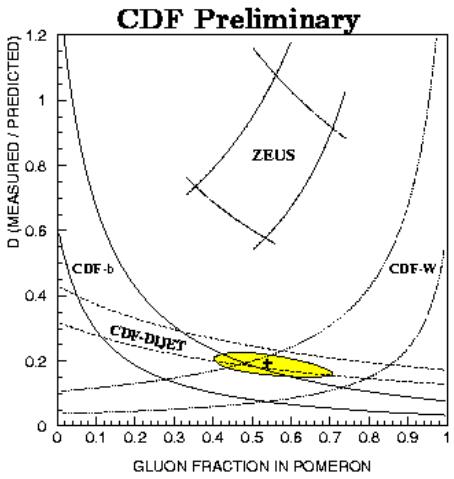

Fig. 6. The ratio, D, of measured to predicted diffractive rates as a function of the gluon content of the Pomeron. The predictions are from POMPYT using the standard Pomeron flux and a hard Pomeron structure.

In 1996 CDF installed three forward proton detectors to be able to tag the diffractively scattered proton. Data was taken at both $\sqrt{s} = 1800\,\mathrm{GeV}$ and $\sqrt{s} = 630\,\mathrm{GeV}$, requiring a good reconstructed track. The forward proton detectors have acceptance for $0.4 < \xi < 0.1$ and $|t| < 1\mathrm{GeV}^2$ at $\sqrt{s} = 1800\,\mathrm{GeV}$ and $|t| < 0.2\mathrm{GeV}^2$ at $\sqrt{s} = 630\,\mathrm{GeV}$. From these data, events are selected with two jets of $E_T \geq 7\,\mathrm{GeV}$, and the momentum fraction of the parton in the pomeron can be measured from

$$\beta = \frac{E_T^{jet1} e^{\eta_1} + E_T^{jet2} e^{\eta_2}}{\sqrt{s}\xi}. \tag{3}$$

After a correction from pile-up background and detector acceptance, the ratio of the data β-distribution in comparison to a Monte Carlo flat gluon structure

is shown in Fig. 7. Although well-described at large β by a flat structure, there is an excess of events at low-β, implying a softer structure component. This is consistent with MC comparisons to data at DØ.

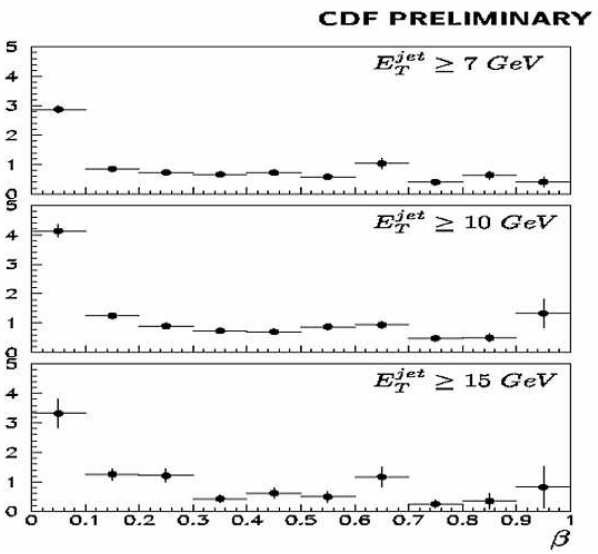

Fig. 7. The ratio of background subtracted data to Monte Carlo simulation using a flat gluon Pomeron structure and standard flux.

3 Hard Double Pomeron Exchange

Hard double pomeron exchange is another process to enable better understanding of diffraction. In the Ingelman-Schlein model, both the incoming proton and anti-proton can be said to "emit" a pomeron and the two pomerons interact to produce a massive system.

The data analysis for HDPE is analagous to hard single diffraction, except that a rapidity gap or forward proton track is required on one side and the diffractive component in the multiplicity on the opposite side is measured. DØ triggers at 1800 GeV (630 GeV) on two 15 (12) GeV jets and a rapidity gap in the LØ detector. Figure 8 shows the opposite multiplicity distributions at 1800 GeV. The distributions at 630 GeV are similar. A clear peak at low multiplicity is observed in both distributions above a flat background in qualitative agreement with expectations for an HDPE signal. Figure 8 also shows the jet E_T distribution for events with two gaps, one gap, and an inclusive distribution. The jet E_T spectra for jets in both kinds of gap events are observed to be similar to the inclusive $p\overline{p}$ scattering. CDF finds similar preliminary results at $\sqrt{s} = 1800$ GeV and measures the rates for hard double pomeron exchange

to be $\sim 10^{-3}/\mathcal{A}_{\mathcal{DPE}}\%$ where the gap acceptance $\mathcal{A}_{\mathcal{DPE}} \sim 0.1$ for two jets with $E_T > 7\,\mathrm{GeV}$ and $0.04 < \xi_{\overline{p}} < 0.1$ [16]. The kinematic properties of DPE candidates are in agreement with expectations events with very little radiation.

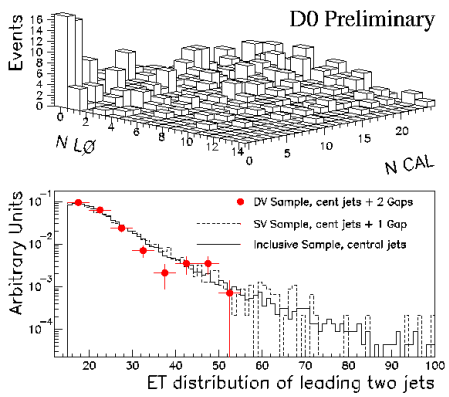

Fig. 8. The multiplicity at 1800 GeV after requiring a rapidity gap on the opposite side. The peak in the low multiplicity bins shows a clear double gap signal. The bottom figure is the corresponding jet E_T distribution for the double gap (*circles*), one gap (*dotted*), and an inclusive jet (*solid*) samples.

4 Hard Color Singlet Exchange

Both experiments have also studied events with a central rapidity gap between jets [13,25–28]. This topology could be due to very large momentum transfer pomeron exchange (a class of double diffractive events), with $|t| >> 100\,\mathrm{GeV}^2$ compared to the previously mentioned processes which typically have $|t| \simeq 0 GeV^2$. The fraction of dijet events with a central rapidity gap is typically on the order of 1%. DØ observes an increase in the gap fraction with transverse energy and pseudorapidity. Comparisions to Monte Carlo show that the data favor a soft color model [29,30], where the hard interaction is a standard QCD exchange and the rapidity gap is generated by a cancellation of the color by soft radiation. The two gluon models for the pomeron do not describe the data well. Although CDF does not observe an increase in the gap fraction with energy and pseudorapidity, the measurements are consistent with DØ.

5 Conclusion

Hard diffraction has been studied and observed at the TEVATRON in three types of processes: single diffraction, double diffraction, and double pomeron exchange at both $\sqrt{\mathrm{s}} = 630$ and $1800\,\mathrm{GeV}$. The analyses at DØ and CDF present consistent

and complimentary results. The diffractive events are quieter in general than ordinary QCD events and the pomeron structure in single diffraction contains a significant soft component. The hard single diffractive and double diffractive gap fractions are $\sim O(1\%)$, which when compared to the HERA results $\sim O(10\%)$, represent a breakdown in the IS factorization. Moreover, there does not appear to be a single scale, dependent on $\sqrt{s}$, between the $p\overline{p}$ and ep experiments.

References

1. M. Derrick et al. (ZEUS Collaboration): Phys. Lett. B **315**, 481 (1993)
2. T. Ahmed et al. (H1 Collaboration): Nucl. Phys. B **429**, 477 (1994)
3. P.D.B. Collins: An Introduction to Regge Theory and High Energy Physics, Cambridge University Press, Cambridge (1977).
4. G. Ingelman, P. Schlein: Phys. Lett. **B152**, 256 (1985)
5. A. Brandt et al (UA8 Collaboration): Phys. Lett. B **297**, 417 (1992)
6. A. Doyle: GLAS-PPE/96-01,*Workshop on HERA Physics, "Proton, Photon, and Pomeron Structure"*.
7. S. Abachi et al. (DØ Collaboration): FERMILAB-CONF-96-247-E, Proceedings of the 28th International Conference on High-energy Physics, Poland (1996)
8. F. Abe et al. (CDF Collaboration): Phys. Rev. Lett. **79**, 2636 (1997)
9. C. Adloff et al. (H1 Collaboration): Eur. Phys. J. **C6**, 421 (1999)
10. J. Breitweg et al. (ZEUS Collaboration): Eur. Phys. J. **C5**, 41 (1998)
11. F. Abe et al. (CDF Collaboration): Phys. Rev. Lett. **78**, 2698 (1997)
12. L. Alvero, J.C. Collins, J. Terron, J. Whitmore: Phys. Rev D **59**, 74022 (1999)
13. S. Abachi et al. (DØ Collaboration): Phys. Rev. Lett. **76**, 734 (1996)
14. H. deKerret et al.: Phys. Lett. B **68**, 385 (1977)
15. D. Joyce et al.: Phys. Rev. D **48** 1943 (1993)
16. K. Borras, *Hard Diffraction at CDF,* Proceedings of the Deep Inelastic Scattering Workshop, Zeuthen Germany(1999)
17. K. Mauritz, *Hard Diffraction at DØ,* Proceedings of the Deep Inelastic Scattering Workshop, Zeuthen Germany(1999)
18. F. Abe et al. (CDF Collaboration): Nucl. Instrum. and Meth. in Phys. Res. A **271**, 387 (1988)
19. S. Abachi et al. (DØ Collaboration): Nucl. Instrum. and Meth. in Phys. Res. A **338**, 185 (1994)
20. T. Affolder et al. (CDF Collaboration): submitted to Phys. Rev. Lett. (1999)
21. P. Bruni, G. Ingelman: Proceedings of the Europhysics Conference on HEP, Marseille, 595 (1993)
22. H.-U. Bengtsson, T. Sjöstrand: Comp. Phys. Comm. **46**, 43 (1987)
23. K. Goulianos: Phys. Lett. B **358**, 379 (1995)
24. J. Collins, *Light-cone Variables, Rapidity and All That,* hep-ph/9705393.
25. S. Abachi et al. (DØ Collaboration): Phys. Rev. Lett. **72**, 2332 (1994)
26. F. Abe et al. (CDF Collaboration): Phys. Rev. Lett. **74**, 855 (1995)
27. B. Abbott et al. (DØ Collaboration): Phys. Lett. **B440**, 189 (1998)
28. F. Abe et al. (CDF Collaboration): Phys. Rev. Lett. **80**, 1156 (1998)
29. G. Ingelman: *Old and New Ideas on Hard Diffraction,* Proceedings of the LISHEP Workshop, Rio de Janerio (1998)
30. O.J.B. Eboli, E.M. Gregores, F. Halzen: *(No) color in QCD: Charmonium, charm and rapidity gaps*, hep-ph/9611258 (1996)